

Chemical Modification of Cellulose Isolated from Underutilized *Hibiscus sabdariffa* via Surface Grafting: A Potential Bio-based Resource for Industrial Application

DOI: 10.15255/KUI.2016.024

KUI-25/2017

Original scientific paper

Received June 12, 2016

Accepted July 29, 2016

A. Adewuyi^{a,b*} and F. Vargas Pereira^b^a Department of Chemical Sciences, Faculty of Natural Sciences, Redeemer's University, 110115 Mowe, Ogun state, Nigeria^b Department of Chemistry, Federal University of Minas Gerais, Av. Antônio Carlos, 6627, Pampulha, CEP 31270-901 Belo Horizonte, MG, Brazil

This work is licensed under a Creative Commons Attribution 4.0 International License



Abstract

Grafting of ethylenediamine onto *Hibiscus sabdariffa* cellulose was achieved via the simple reaction mechanism. The modified *Hibiscus sabdariffa* cellulose (HSM) and unmodified *Hibiscus sabdariffa* cellulose (HSC) were characterized using Fourier transformed infrared (FTIR) spectroscopy, elemental analysis, scanning electron microscopy (SEM), X-ray diffraction (XRD), particle size distribution, zeta potential, thermogravimetric analysis (TGA), and differential scanning calorimetry (DSC). Both HSM and HSC were also analysed for their water holding capacity, oil holding capacity, swelling capacity, and heavy metal adsorption capacity. The particle size distribution of HSC was found to be monomodal, while that of HSM was bimodal. HSM performed better than HSC in terms of oil adsorption capacity and metal adsorption capacity especially for Pb²⁺ and Cd²⁺ ions. HSM also performed better than some reported cellulosic materials found in literature. These properties exhibited by HSM present it as a potential resource in the food industry and in treatment of heavy metal contaminated water.

Keywords

Cellulose, ethylenediamine, *Hibiscus sabdariffa*, modified cellulose, surface grafting

1 Introduction

Cellulose is a polysaccharide with numerous applications. It is usually described as a complex carbohydrate and well known as the most abundant polymer on Earth.^{1,2} Plants, most especially wood, have been the major sources of cellulose. With the current high demand for materials, energy, and food face-to-face with the growing world population, there is a need to search for much more convenient sources that can serve as alternatives or means of relief for the presently known sources of cellulose.

Underutilized plant materials are possible sources of alternative means of relief for conventional sources of cellulose such as cottonseed and wood. It is important to screen some of these underutilized plants, especially the seeds, for their cellulose content and characterize them. The *Hibiscus sabdariffa* seed (HS) is an example of an underutilized plant material with the potential of being a suitable source of cellulose. *Hibiscus sabdariffa* belongs to the Malvaceae plant family; it is a shrub usually regarded as perennial. The leaf is known for some uses, which cut across food and medicine.^{3–5} Presently in Nigeria, the seeds of *Hibiscus sabdariffa* are considered underutilized and are regarded as waste, although there have been reports that oil from the seed has properties similar to that of crude olive oil⁶ while other reports have shown that the oil is nonedible.⁷

Cellulose is capable of being used as an industrial feedstock for the production of known conventional or emerging bio-

based products. The search for such bio-based products or feedstock has been a global challenge. With the current instability in petroleum, global warming, and other environmental issues, bio-based products and feedstock can be considered green, and will be of tremendous benefit to man and the environment. A cellulose-based product or feedstock can serve as a green resource with numerous benefits. The performance of cellulose may be improved by simple chemical modification, although different modification has been reported in the past;^{8–10} but there is the need for a cheap, green, and simple process of modification using underutilized plants as sources of cellulose.

As a semicrystalline polymer, with both crystalline and amorphous phases, that contains two types of hydrophilic hydroxyl groups [which are primary hydroxyl in methylol group (–CH₂OH) at C-6 and secondary hydroxyl groups (–OH) at C-3 and C-4],¹¹ it can be modified chemically. Grafting is a method which can be used to modify the surface of cellulose.¹² Such modification may improve certain properties of the cellulose, such as elasticity, hydrophilic character, water and oil adsorption capacity, thermosensitivity, heat resistance, antimicrobial capacity, ion-exchange capacity, pH sensitivity, and crystallinity.^{13–16} Surface-grafted cellulose is presently finding application in water treatment, medicine, personal care products, textile, and food industries.¹⁷ This has created the need and search for cheap, environmentally friendly, and efficient biopolymers from natural resources like cellulose.

In response to this, the present study has focused on the chemical modification of cellulose isolated from *Hibiscus sabdariffa* via surface grafting. The properties of the raw

* Corresponding author: Adewale Adewuyi
email: walexy62@yahoo.com

cellulose and the surface-grafted cellulose were determined, compared, and examined for possible environmental applications.

2 Experimental

2.1 Materials

The seeds of *Hibiscus sabdariffa* were obtained from a garden in Ibadan, Oyo state, Nigeria. This was later identified at the Department of Botany and Microbiology, University of Ibadan, Ibadan, Oyo state, Nigeria. The seeds were ground in an industrial mill, extracted with hexane as previously described by Adewuyi *et al.*,¹⁸ air dried, and stored in an airtight container. Sodium chlorite, sodium hydroxide, acetic acid, chloroacetic acid, thionyl chloride, ethylenediamine, and all other chemicals used in this study were purchased from Sigma-Aldrich (Brazil) and are of Analar grade.

2.2 Isolation of cellulose from the seed of *Hibiscus sabdariffa*

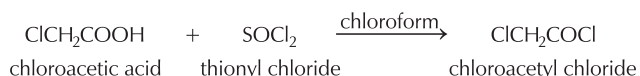
An amount of 200 g of defatted *Hibiscus sabdariffa* seed sample (hexane extracted) was weighed and transferred into a 4 L beaker. Alkali solution (mass fraction of NaOH 2 %) was added and heated at 80 °C for 5 h with continuous stirring using a Fisatom mechanical stirrer. The mixture was later filtered and washed with distilled water several times until alkali-free, and oven-dried at 50 °C. The treatment with 2 NaOH was repeated twice. The brown product obtained was bleached with a mixture of solution made up of equal volumes (1 : 1) of acetate buffer (27 g NaOH

and 75 mL glacial acetic acid, diluted to 1 L of distilled water), and aqueous sodium chlorite (mass fraction of NaClO₂ 1.7 % in distilled water), as described by Flauzino Neto *et al.*¹⁹ This was stirred at 80 °C for 5 h.

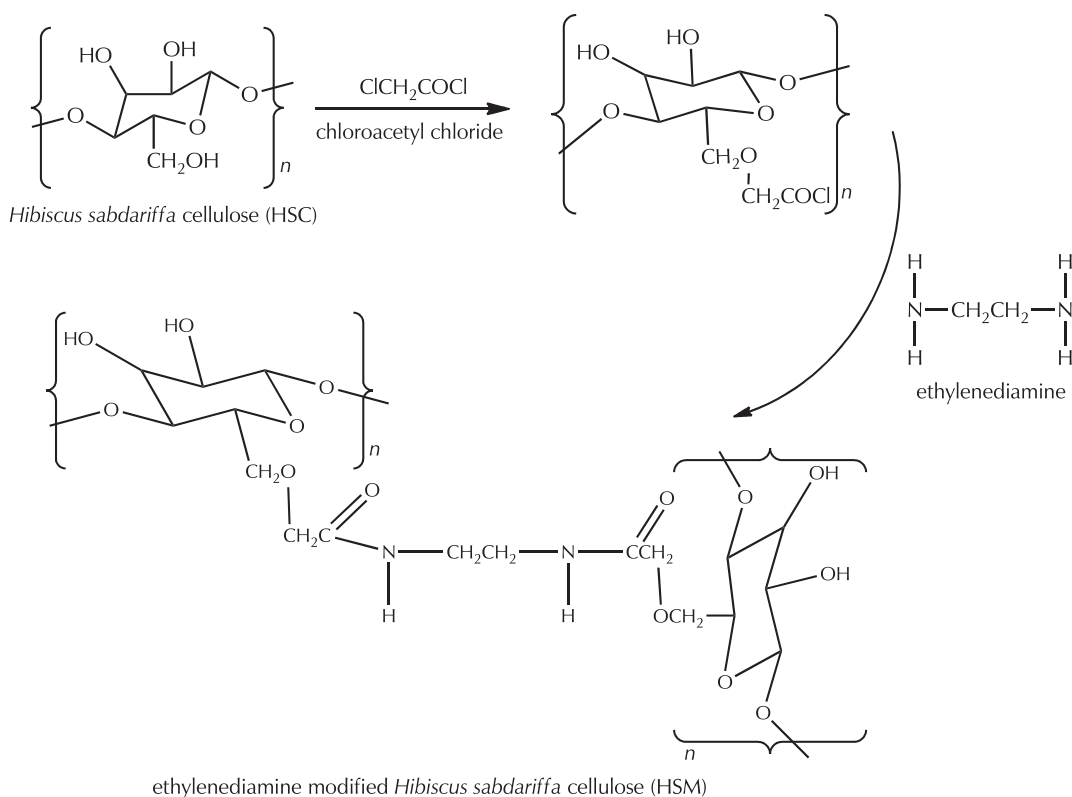
The resulting fibres were washed repeatedly in distilled water until the fibres became neutral. The bleaching step was repeated twice until the fibre became completely white, and dried in an air-circulating oven at 50 °C for 24 h.

2.3 Modification of *Hibiscus sabdariffa* cellulose

A mixture of chloroacetic acid (0.03 mol), thionylchloride (0.04 mol), and chloroform was heated to 75 °C for 30 min to form chloroacetyl chloride, as described in scheme 1a. An amount of 8.35 g of *Hibiscus sabdariffa* cellulose (HSC) was added to the chloroacetyl chloride (after the removal of excess thionyl chloride under reduced pressure); this was allowed to react for 5 h under constant stirring at 100 °C, and finally cooled in ice. Ethylenediamine (30 ml) was added and stirred for 12 h at 100 °C under reflux. Cold distilled water was added to the mixture, and centrifuged thrice for 10 min at 8500 rpm to remove excess ethylenediamine. The orange coloured product (HSM) obtained was then dried at 50 °C for 24 h. The reaction scheme is shown in Scheme 1b.



Scheme 1a – Synthesis of chloroacetylchloride



Scheme 1b – Modification of *Hibiscus sabdariffa* cellulose

2.4 FTIR spectroscopy

The functional groups in HS, HSC, and HSM were determined using FTIR (Perkin Elmer, spectrum RXI 83303). The samples were blended with KBr, pressed into pellets, and analysed in the range of 400–4500 cm^{-1} .

2.5 Elemental analysis

Elemental analysis of HSC and HSM was achieved using Perkin Elmer series II CHNS/O analyser (Perkin Elmer, 2400, USA).

2.6 Scanning electron microscopy

Surface morphology was studied using scanning electron microscope (SEM, JEOL JSM-6360LV, Japan). Powdered HS, HSC, and HSM were coated with gold using the sputtering technique in order to increase electrical conductivity and the quality of the micrographs.

2.7 X-ray diffraction analysis

The X-ray diffraction pattern was obtained using X-ray diffractometer (XRD-7000X-Ray diffractometer, Shimadzu) with filtered $\text{Cu K}\alpha$ radiation operated at 40 kV and 40 mA. The XRD pattern was recorded from 10 to 80° (2θ), with a scanning speed of 2.00° per minute. The crystallinity index (I_c) was determined using the height of 200 peak (I_{002} , $2\theta = 22.5^\circ$), and the minimum intensity between the 200 and 110 peaks (I_{AM} , $2\theta = 18^\circ$) which can be expressed as:

$$I_c = \frac{I_{002} - I_{AM}}{I_{002}} \quad (1)$$

where I_{002} represents both crystalline and amorphous material, while I_{AM} represents the amorphous material only.

2.8 Particle size distribution and zeta potential

HSC and HSM were analysed for their particle size distribution and zeta potentials using a zeta potential analyser (DT1200, Dispersion technology) at 25 °C while observing general calculation model for irregular particles. Several measurements were taken using Dispersion technology-AcoustoPhor Zetasize 1201 software (version 5.6.16).

2.9 Thermal stability

Thermal stability and fraction of volatile components of HS, HSC, and HSM were monitored by TGA, DTA, and DTG. This was achieved using a simultaneous DTA-TG apparatus (SHIMADZU, C30574600245).

2.10 Water holding capacity

The water holding capacity (WC) was determined as described by Zhang et al.²⁰ To achieve this, 0.5 g (W_1) of

sample was dispersed in 10 mL of distilled water in pre-weighed, clean centrifuge tubes (W) placed in a water bath at 37 °C for 30 min. These were centrifuged for 15 min at 4000 rpm; the supernatant was removed and the centrifuge tubes with the distilled water soaked samples were weighed (W_2). The water holding capacity was estimated as:

$$WC = \frac{W_2 - (W + W_1)}{W_1} \quad (2)$$

2.11 Oil holding capacity

The oil holding capacity (OC) was determined by weighing 0.2 g (W) of samples into a calibrated centrifuge tube containing 5 ml (V_1) of *Picralima nitida* seed oil. The mixture was properly stirred for 10 min, after which it was centrifuged for 30 min at 5000 rpm. The supernatant oil (V_2) was gently removed while the absorbed oil was estimated as the difference between V_1 and V_2 . The oil holding capacity was calculated as described by Lu et al.²¹:

$$OC = \frac{V_1 - V_2}{W} \quad (3)$$

2.12 Swelling capacity

Both the HSC and HSM were separately analysed for their swelling capacity (SC) by accurately weighing 0.5 g (W) and placing it in a calibrated tube, measuring its initial bed volume (V_3), mixed with 10 ml of milliqui water and shaken vigorously. The tube with its content was placed in a water bath at 25 °C for 24 h, the final volume (V_4) measured, and the swelling capacity calculated using Eq. 4.²²

$$SC = \frac{V_4 - V_3}{W} \quad (4)$$

2.13 Heavy metal adsorption capacity

Lead(II) nitrate ($\text{Pb}(\text{NO}_3)_2$), cadmium sulphate ($3\text{CdSO}_4 \cdot 8\text{H}_2\text{O}$), and copper(II) sulphate ($\text{CuSO}_4 \cdot 5\text{H}_2\text{O}$) salts were used in the preparation of the salt solutions in milliqui water. Metal adsorption study was carried out by separately shaking 0.1 g of HSC and HSM with 50 ml of solutions (100 mg l^{-1}) of metal in different beakers at 25 °C and 200 rpm for 3 h. This was later centrifuged for 10 min at 5000 rpm, and the metal concentrations before and after adsorption were determined using Atomic Absorption Spectrometer (Varian AA240FS). The metal ions adsorption capacity of HSC and HSM were calculated using equation:

$$q_e = \frac{(c_o - c_e)V}{m} \quad (5)$$

where q_e is the adsorption capacity, c_o and c_e are initial and final concentrations of adsorbate (Pb^{2+} , Cd^{2+} and Cu^{2+}) in solution, respectively; while V and m are volume of metal ions solution and mass of HSC and HSM used.

3 Results and discussion

3.1 FTIR spectroscopy

The cellulose yield from the seed of *Hibiscus sabdariffa* was 23.31 %, while the grafting process gave rise to a product (HSM) yield of about 92 %. The photo images of HS, HSC, and HSM are shown in Fig. 1, while the FTIR spectra are presented in Fig. 2. The spectrum of HS revealed bands at 1742, 3430, and 2946 cm^{-1} , which may be attributed to the vibrational frequencies of ester functional group ($-\text{COOR}$), hydroxyl functional group ($-\text{OH}$), and alkane group ($\text{C}-\text{H}$), respectively. The presence of the peak observed at 1752 cm^{-1} may be attributed to the presence of other carbonyl functional group in HS, while the peak at 1101 and 1030 cm^{-1} represents the $\text{C}-\text{O}-\text{C}$ stretching of lignin and $\text{C}-\text{O}$ vibrational stretching of cellulose and hemicellulose, respectively.²³

After the treatment with 2 % NaOH and bleaching, the peak attributed to the ester functional group disappeared with HSC and HSM exhibiting a broad band in the region 3530–3210 cm^{-1} , which indicates the presence of free $\text{O}-\text{H}$ stretching vibration of the OH functional groups in both HSC and HSM molecules. The presence of the OH functional groups in the spectrum of HSM suggests that most modification reactions in the cellulose occurred preferably on the amorphous regions due to the high reactivity and accessibility of the amorphous regions^{24,25}, leaving behind the OH groups in the crystalline region.

Both samples had peaks at 1040 cm^{-1} which may be due to the $\text{C}-\text{O}-\text{C}$ pyranose ring stretching vibration.²⁶ The absorption band at 904 cm^{-1} in HSC and HSM was assigned to the stretching at β -(1 \rightarrow 4) glycosidic linkages. Peaks found at 2892 cm^{-1} and 1365 cm^{-1} in HSC and HSM were considered to be the characteristic $\text{C}-\text{H}$ stretching

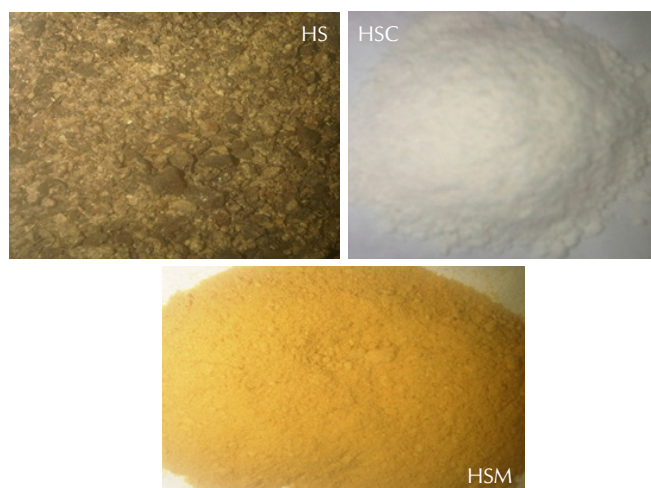


Fig. 1 – Photo images of *Hibiscus sabdariffa* ground seed (HS), cellulose (HSC), and modified cellulose (HSM)

vibrational frequency, and bending vibration of $\text{C}-\text{H}$ and $\text{C}-\text{O}$ bonds in the polysaccharide aromatic rings, respectively; while the bands in the region 1651–1640 cm^{-1} were accounted for as being the $\text{O}-\text{H}$ bending of the adsorbed water.^{27,28} The vibrational frequencies found at 1161 cm^{-1} and 1100 cm^{-1} were assigned to the $\text{C}-\text{C}$ ring breathing band and $\text{C}-\text{O}-\text{C}$ glycosidic ether band from the polysaccharide component, respectively. These two peaks became more pronounced in HSM, which may be due to the copolymer amide linkage formed in HSM from the ethylenediamine modification, as shown in Scheme 1b. The amide peaks in HSM were found at 1320 cm^{-1} and 1530 cm^{-1} ; the peak at 1530 cm^{-1} was attributed to the $\text{N}-\text{H}$ bending vibrations coupled with $\text{C}-\text{N}$ vibration of the amide formed in HSM.

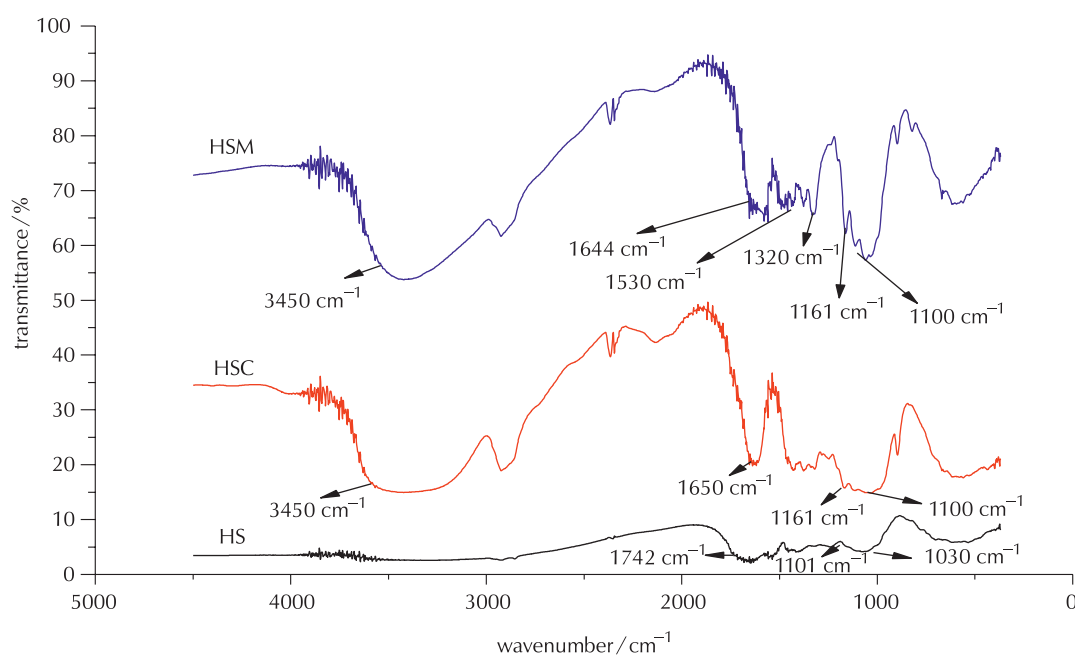


Fig. 2 – FTIR spectra of *Hibiscus sabdariffa* seed (HS), cellulose (HSC), and modified cellulose (HSM)

Also, the absorption band around 1450 cm^{-1} was attributed to the symmetric CH_2 bending vibrations, which are also considered to be the “crystallinity band”.²⁹ The FTIR result was further used to calculate the empirical crystallinity index (ECI), which was proposed as the lateral order index by Nelson and O’Connor.³⁰ This was achieved using the expression which we have modified to be in percent-age:

$$\text{ECI} = \frac{A_{1430\text{ cm}^{-1}}}{A_{897\text{ cm}^{-1}}} \quad (6)$$

The band at 1430 cm^{-1} was attributed to the crystalline structure of the cellulose, while the band at 897 cm^{-1} was assigned to the amorphous region of the cellulose. Nelson and O’Connor defined the ratio of these bands as the empirical crystallinity index, as shown in Eq. 6. The ECI value of HS was 42.51 %, that of HSC was 65.24 %, while it was calculated to be 61.00 % in HSM %. The ECI is an overall expression of the degree of order in the structure of HS, HSC, and HSM;³¹ this has shown that HSC and HSM have better ordered structures than HS which is the raw *Hibiscus sabdariffa* seed.

3.2 Elemental analysis

The CHN analysis revealed the presence of carbon, hydrogen, and nitrogen in HSC. The percentage composition of these elements was found higher in HSM than in HSC. After the modification, the composition of carbon increased from 48.28 % in HSC to 51.96 % in HSM, hydrogen increased from 10.33 % in HSC to 13.05 % in HSM, while nitrogen was found to be 0.12 % in HSM. The increase in the amounts of these elements showed that modification had taken place in the cellulose.

3.3 Scanning electron microscopy

The SEM images of HS, HSC, and HSM are shown in Fig. 3. The surface morphology of HS appeared to have a diameter considerably larger than those found for HSC and HSM, and it seemed to be composed of several microfibrils with each fibre having a compact structure. The micrograph also showed that the surface of HS was not entirely smooth, which may be due to the presence of some functional groups at this surface. The surface micrograph of HSC was different from that of HS with a reduction in diameter which may have resulted from the removal of lignin, hemicellulose and other non-cellulosic constituents. The reticular structure of HSC indicated that the process of purifying and bleaching had not broken the cellulose structure.³² Moreover; the surface of HSC also exhibited a lumpish structure, which may be due to the strong intramolecular hydrogen bonds that exist in the molecule. On the other hand, the somewhat smooth surface of HSM revealed that the introduction of ethylenediamine units into cellulose units of HSC may have limited the formation of the intramolecular hydrogen bonds. The surface of HSM changed remarkably, and was different from those of HS and HSC.

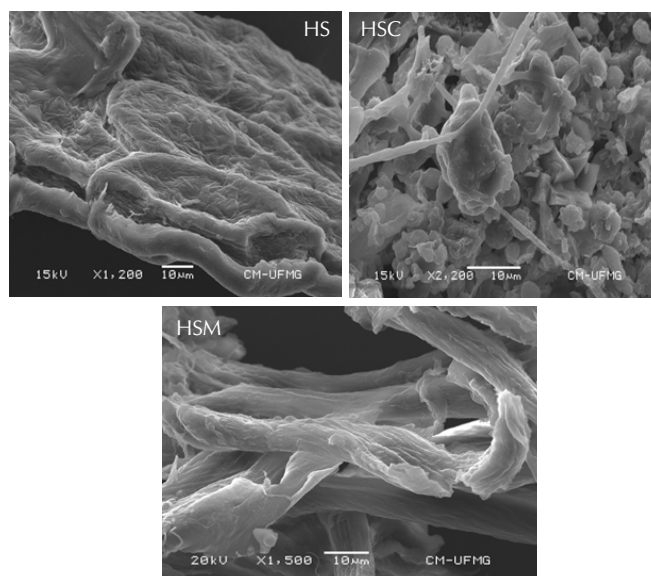


Fig. 3 – SEM images of *Hibiscus sabdariffa* seed (HS), cellulose (HSC), and modified cellulose (HSM)

3.4 X-ray diffraction analysis

The X-ray diffractogram of HS, HSC, and HSM are presented in Fig. 4. It is evident that the diffractograms of HSC and HSM exhibited sharp peaks at around 18° and 22.5° 2θ angles; these peaks were attributed to the diffraction planes of 110 and 002^{33,34} such are typical of cellulose I crystal form; moreover, there was no doublet in the main peak at 2θ (22.5°). The crystallinity index of HS was found to be 24.74 %, this value increased in HSC to 59.03 %, and 59.17 % in HSM, suggesting an increase in the intra- and intermolecular hydrogen bonding, which occurs as amorphous HS is transformed into cellulose I. This closely related value of crystallinity index of HSC and HSM corroborates the observation from the FTIR result of similar intensity at absorption band around 1450 cm^{-1} in HSC and HSM, although there was a slight increase in the crystallinity index of HSM over that of HSC, indicating the likelihood of higher water resistance in HSM, since water absorption occurs mainly in the amorphous region of a polymeric molecule.³⁵ The lower crystallinity index of HS may be due to the presence of higher amorphous content when compared to HSC and HSM, while the higher crystallinity observed in HSC and HSM may also be attributed to the removal of lignin, hemicellulose, and other non-cellulosic substances.³⁶

3.5 Particle size distribution and zeta potential

Particle size is one of the vital parameters in materials science, which cuts across engineering, biology, medicine, energy, pharmacy, geosciences and technology. The particle size distribution and zeta potential of HSC and HSM are presented in Fig. 5. The particle size distribution of HSC and HSM were found to be monomodal with a mean size of 10.240 and 10.138 , respectively.

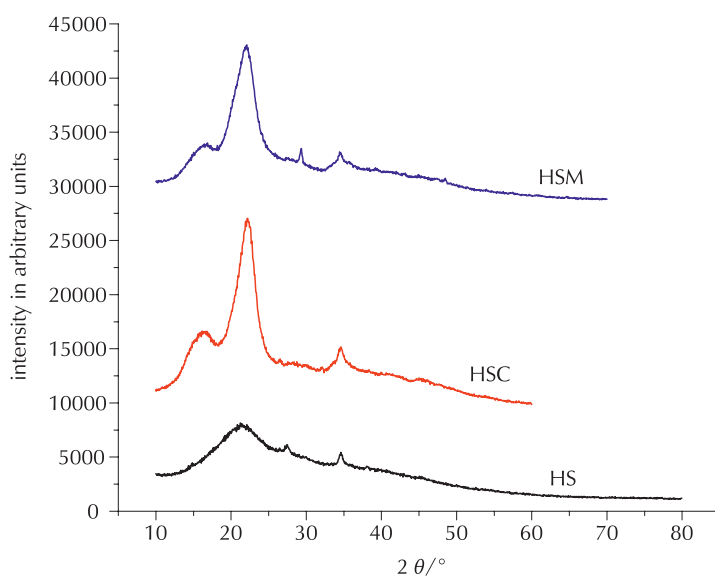


Fig. 4 – X-ray diffraction patterns of *Hibiscus sabdariffa* seed (HS), cellulose (HSC), and modified cellulose (HSM)

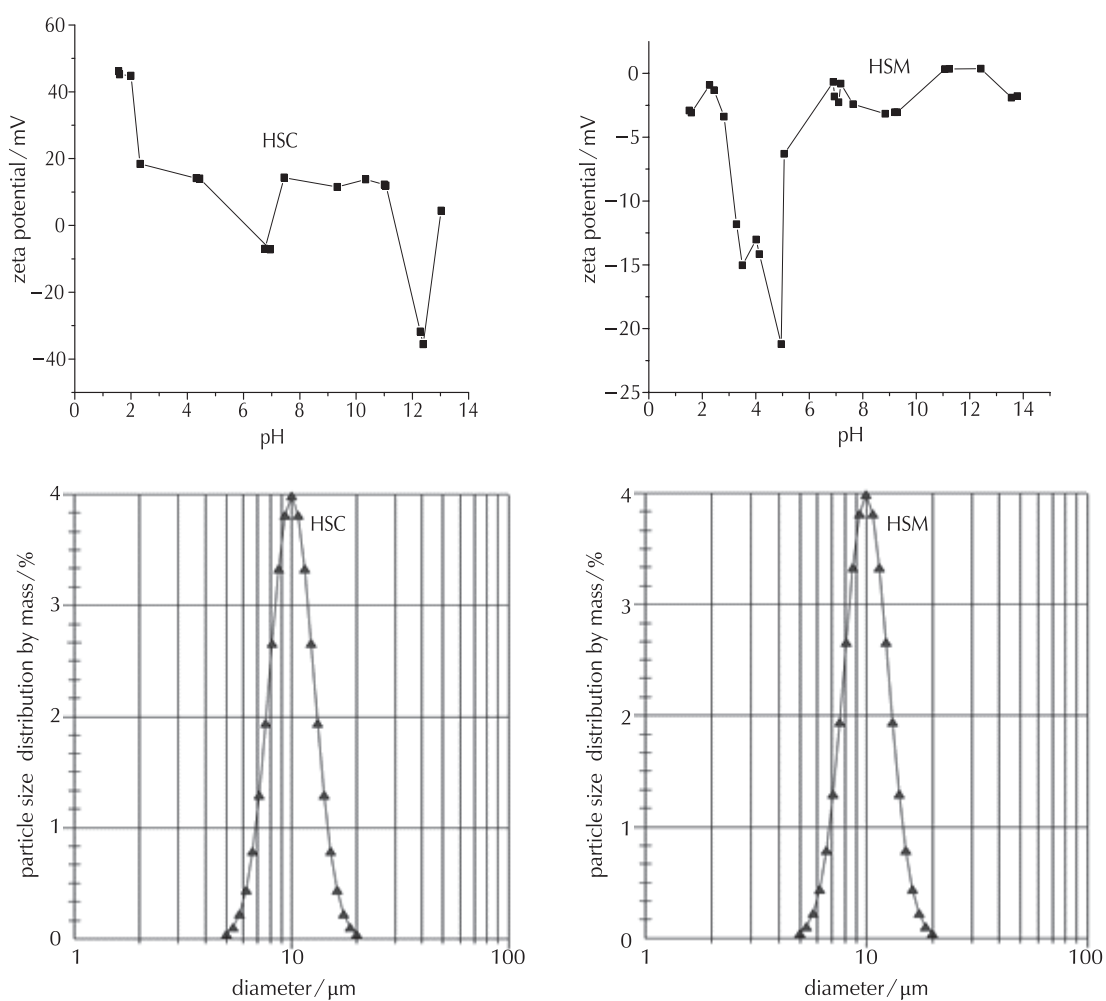


Fig. 5 – Zeta potential and particle size distribution of HSC and HSM

The zeta potential of HSC mainly reduced as the pH increased, whereas HSM maintained a higher zeta potential than HSC even at high pH. The lowest zeta potential was found at pH 5 in HSM, and at pH 11 in HSC. The values of the zeta potential helped in quantifying the charges at the surfaces of HSC and HSM³⁷, which indicates the degree of HSC and HSM stability and electrostatic repulsion with other charged particles;³⁸ this goes a long way in finding suitable applications for materials. As pointed out by *Salopek et al.*,³⁹ the distribution of the zeta potential at various pH along the surfaces of HSC and HSM showed that these materials are stable in liquid medium (solid-liquid interaction).

3.6 Thermal stability and Brunauer-Emmett-Teller surface area analysis

The TG and DTG curves of HS, HSC, and HSM are shown in Fig. 6. These curves reveal an initial loss in mass between 48 °C and 112 °C, which may be associated with loss of water molecules in these samples; this is likely the chemisorbed water found at around 1651–1640 cm^{-1} in the FTIR spectra. HS showed two distinct stages, HSC showed three, while HSM showed four different stages of mass loss during decomposition. An increase was noticed in the region of water loss (up to 110 °C) for HSC with respect to HS and HSM; this may be considered to be due to the higher extent of solvation or ionic interaction around the cellulose molecules with the water molecules. The amorphous region of the cellulose may have also provided enhanced interchain spaces where water molecules could have been picked up or trapped. Better still, water molecules may have been picked up in vacant spaces left on HSC after the removal of hemicellulose and lignin. Cellulose has been reported to degrade mainly by dehydration, depolymerisation, and glucosan formation.⁴⁰ The first stage of mass loss noticed in HSC was around 170–220 °C, which can be attributed to degradation leading to 1,4 and 1,6 anhydroglucopyranoside, while the second stage at 342 °C could be considered as being depolymerization at

1,4 glycosidic bond, as previously reported.^{41,42} Pyrolysis to lower molecules was found at higher temperatures, which was the third stage. A similar degradation mechanism was also found in HSM except for the appearance of a peak around 260 °C. The first stage of loss in mass was observed at around 150–210 °C in HS, this weight loss was accounted for as being loss of hemicellulose and some other volatile matter. Loss of weight at around 220–450 °C in HS was considered as being due to loss of lignocelluloses⁴³, while the loss found at temperatures above 450 °C was taken to be due to the loss of lignin and char.^{44,45}

3.7 Water holding capacity

The ability of materials to hold added water along with their own water when undergoing processing is very important. The water holding capacity of HSC and HSM are presented in Table 1. The water holding capacity of HSM was found lower than that of HSC, which may be due to the modification carried out on HSC. This modification may have broken the reticulation of HSC.⁴⁶ The higher water holding capacity of HSC over HSM suggests the possible use of HSC in food applications requiring moisture retention as low-calorie bulk ingredients³⁴, whereas HSM may have potential applications in fields such as paper and pulp, water treatment (adsorbents), and pigments, where low moisture retention is required. Water holding capacity of materials is dependent on several factors such as inherent chemical and physical structure.⁴⁷ The water holding capacity of a food additive or food itself plays a key role in its stability, texture, microbial safety, production costs, and functional properties.⁴⁸ Although good water holding capacity is a necessity for stability and texture, it is important to consider microbial activity and safety which may affect shelf life. Therefore, adequate consideration will have to be taken when selecting materials for water retention in the final product. To this effect, HSM may also be of importance in fields or products where low or moderate water retention is required.

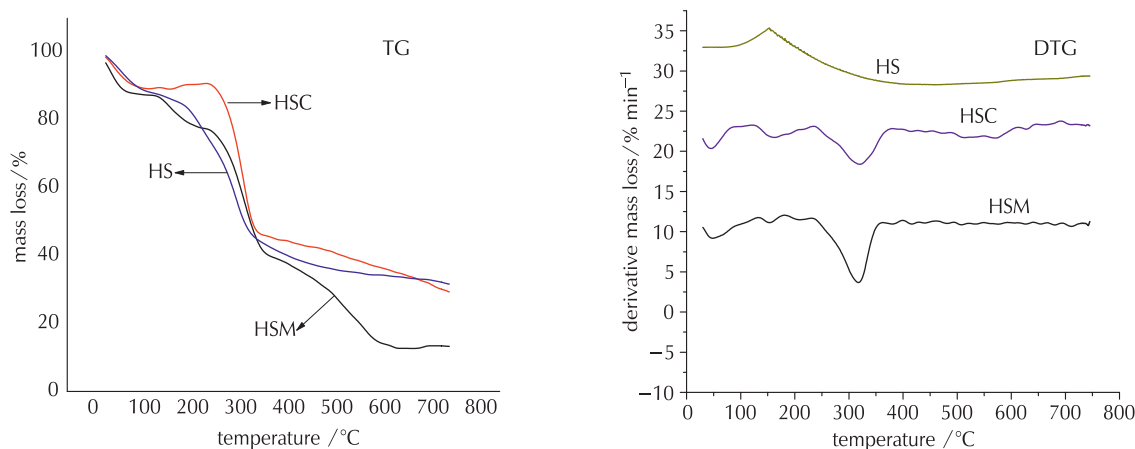


Fig. 6 – TG and DTG curves of *Hibiscus sabdariffa* seed (HS), cellulose (HSC), and modified cellulose (HSM)

Table 1 – Water holding capacity, oil holding capacity, and swelling capacity of HSC and HSM

Sample	WC/gg ⁻¹	OC/mlg ⁻¹	SC/mlg ⁻¹
HSC	11.87	4.59	13.72
HSM	5.55	7.27	1.85

3.8 Oil holding capacity

The oil holding capacity of HSM (7.27 ml g⁻¹) was higher than that of HSC (4.59 ml g⁻¹). The introduction of amide linkage (Scheme 1b) from the modification might have increased the porosity and superficial area of HSM, which could have promoted the entrapment of oil in the HSM molecule.⁴⁹ Oil holding capacity has been related to the adsorption of organic compounds to the surface of the substrates, which in part also relates to the chemical composition that concerns mainly the porosity of the fibre structure of the substrate^{50,51}. This claim further supports the SEM result which reveals the surface of HSC to be of a more compact structure than HSM. *Good oil holding capacity is an important parameter in the food industry which is required in baked goods and soups, meat replacers and extenders, ground meal formulation and doughnuts.*⁵² It is closely related to texture and other food quality properties through the interaction between oil and other components.⁵³ The ability of HSM to absorb and retain oil is important in food formulations; this shows that HSM may find application as an ingredient or additive over HSC in areas requiring oil retention. The higher oil holding capacity of HSM also indicates its enhanced hydrophobic character⁵⁴ which plays an important role in ground meat formulations and shelf life.⁵⁵

3.9 Swelling capacity

The swelling capacity of any cellulosic fibre is considered as the amount of liquid that can be absorbed by such cellulosic fibre. It is an important property that helps in finding useful applications for cellulosic fibres. The swelling capacity of HSC (13.72 ml g⁻¹) is higher than that of HSM (1.85 ml g⁻¹), as shown in Table 1, indicating higher tendency of HSC to hold water molecules. Some of the hydroxyl functional groups in HSC were involved in the grafting process to form HSM, indicating that the hydroxyl group content of HSC is higher than that of HSM. So the high hydroxyl group content of HSC may have aided the interaction with water molecule, and as such giving it a higher hydration property over HSM.

Table 2 shows the comparison of the water holding capacity, oil holding capacity, and swelling capacity of HSC and HSM with other reported values in literature. The oil holding capacity value of HSM was higher than all other values presented in Table 2. The water holding capacity value of HSM also compared favourably with values previously reported, except for values by Nassar *et al.*,⁵⁶ Aydin and Gocmen,⁵⁷ and Yalegama *et al.*⁵¹, which were higher than the value obtained for HSM, while the swelling capacity found in literature were all higher than that of HSM, an observation which was contrary in the case of HSC which had a value higher than all that were found in literature.

Table 2 – Comparison of the water holding capacity, oil holding capacity, and swelling capacity of HSC and HSM with other reported values in literature

Sample	WC/gg ⁻¹	OC/mlg ⁻¹	SC/mlg ⁻¹
standard flour ⁶⁸	1.02	2.50	4.00
red bean flour ⁶⁹	4.419	4.553	–
white lupin ⁵²	2.65	1.82	–
orange peel ⁵⁶	13.60	6.80	–
pumpkin flour ⁵⁷	0.92	2.11	–
gelatin ⁵³	8.59	0.67	–
coconut kernel ⁵¹	8.13	4.57	5.50
cowpea ⁷⁰	2.00	0.80	5.50
HSC (present study)	11.87	4.59	13.72
HSM (present study)	5.55	7.27	1.85

3.10 Heavy metal adsorption capacity

Heavy metals such as Cu²⁺, Cd²⁺ and Pb²⁺ are known to be toxic to humans, plants, and the environment⁵⁸ as they are capable of causing diseases and various disorders. These heavy metals have been found in water, food, and soil as a result of rapid population growth, domestic activities, agricultural practices and industrialization, which leads to waste generation containing these heavy metals.⁵⁹ It is important that these heavy metals are removed from waste before they get into the environment in order to avoid or prevent plants, animals, and humans from coming into contact with these toxic metals. In this line, HSC and HSM were evaluated for their capacity to adsorb heavy metals (Pb²⁺, Cd²⁺ and Cu²⁺ ions). The adsorption capacities of HSC and HSM are shown in Fig. 7. HSC showed higher adsorption capacity for Cu²⁺ ions over HSM, whereas the adsorption capacity of HSM towards Pb²⁺ and Cd²⁺ was higher than those of HSC. The adsorption capacity of HSC for Cu²⁺ was 7.44 mg g⁻¹ while HSM was 6.12 mg g⁻¹. This adsorption capacity is higher than those reported by Tiwari *et al.*,⁶⁰ Wahi *et al.*,⁶¹ Jiang *et al.*,⁶² and Putra *et al.*⁶³ which were 1.67, 1.22, 0.84, and 3.89 mg g⁻¹, respectively. In the case of Pb²⁺ ions, the adsorption capacity was found to be 20.85 mg g⁻¹ for HSM, and 19.63 mg g⁻¹ for HSC, indicating HSM having preference for Pb²⁺ ions over HSC. Aside the adsorption capacity shown by HSM being higher than that of HSC, it was also higher than those reported by Adediran *et al.*,⁶⁴ Jiang *et al.*,⁶² Lawal *et al.*,⁶⁵ and Fitalan *et al.*⁶⁶, which were 5.01, 2.35, 4.86, and 15.00 mg g⁻¹, respectively. Adsorption capacity towards Cd²⁺ was 6.88 mg g⁻¹ for HSM, and 4.58 mg g⁻¹ for HSC, which also presented HSM as having a better adsorption of Cd²⁺ ions. It is obvious from the results that both HSC and HSM demonstrated strong adsorption capacity towards Pb²⁺ ions; the presence of hydroxyl functional group in HSC, and presence of both hydroxyl and amide functional group in HSM may have been responsible for their ability to adsorb heavy metals such as Pb²⁺, Cd²⁺ and Cu²⁺.

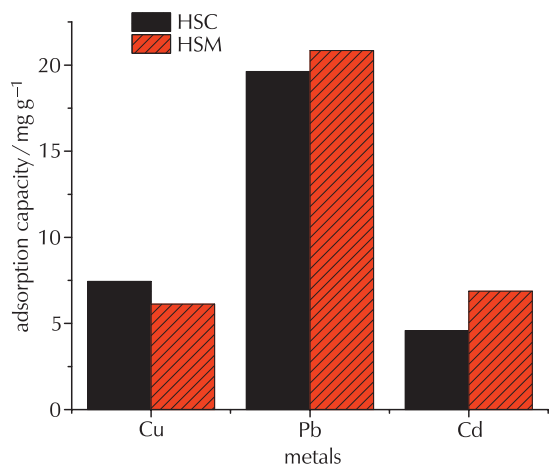


Fig. 7 – Adsorption capacity of HSC and HSM

The mechanism of adsorption of Pb^{2+} , Cd^{2+} and Cu^{2+} ions demonstrated by HSC and HSM may be accounted for as being through ion exchange, or complex action; it may also be due to both ion exchange and complex actions taking place at the same time.³⁴ Aside the functional groups, both HSC and HSM have a network-structure, which is much more compact in the case of HSC than in HSM; thus, from their network-structure, they also have the tendency of being able to trap metal ions.

The percentage amount of metals adsorbed by HSC and HSM are shown in Fig. 8. Both HSC and HSM exhibited low adsorption towards Cu^{2+} and Cd^{2+} ions, but reasonable adsorption towards Pb^{2+} ions with HSC adsorbing 73.49 % of Pb^{2+} ions from solution, while HSM adsorbed 78.10 % of Pb^{2+} ions from solution. This high tendency to adsorb Pb^{2+} better than Cu^{2+} and Cd^{2+} may be due to the differences in the ionic radii of the metals. The ionic radius of Pb^{2+} (1.19 Å) is higher than those of Cd^{2+} (0.95 Å) and Cu^{2+} (0.73 Å), as reported by Wells.⁶⁷ The larger ionic radius of Pb^{2+} ion over Cu^{2+} and Cd^{2+} ions may have resulted in better interaction between Pb^{2+} ions and the surfaces of the HSC and HSM, since the outer shell electrons of Pb^{2+} are more available for bonding than those of Cu^{2+} and Cd^{2+} . The high capacity of HSM towards these heavy metals may be due to the presence of both hydroxyl and amide functional groups, unlike HSC with just hydroxyl groups (Scheme 1b). This exhibited capacity suggests its potential use as an adsorbent ingredient in products requiring adsorption of heavy metals or as a promising adsorbent for heavy metal removal in water treatment.

4 Conclusion

The study focused on the chemical modification of cellulose isolated from *Hibiscus sabdariffa* via surface grafting. The chemical and functional properties of unmodified *Hibiscus sabdariffa* cellulose and modified *Hibiscus sabdariffa* cellulose were compared with earlier works reported in literature. The examined properties of modified *Hibiscus sabdariffa* cellulose performed better than that of unmod-

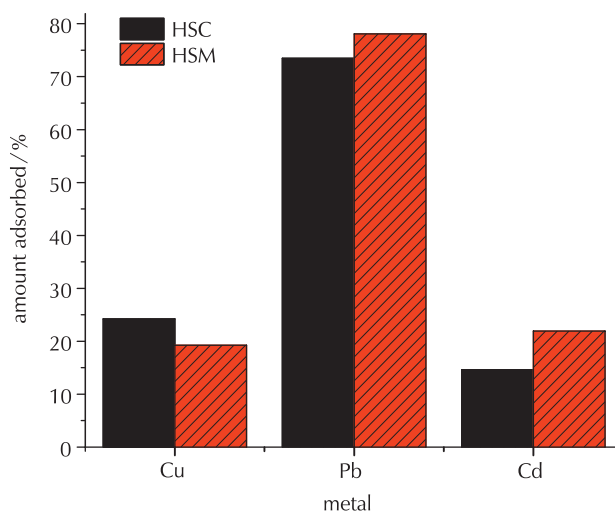


Fig. 8 – Adsorption of Cu^{2+} , Pb^{2+} and Cd^{2+} on HSC and HSM

ified *Hibiscus sabdariffa* cellulose in terms of oil adsorption capacity and metal adsorption, especially Pb^{2+} and Cd^{2+} ions. The modified *Hibiscus sabdariffa* cellulose also performed better than some reported cellulosic materials found in literature. These exhibited properties of the modified *Hibiscus sabdariffa* cellulose indicated that the modified *Hibiscus sabdariffa* cellulose has the potential of finding application in the food industry and treatment of heavy metal contaminated water.

ACKNOWLEDGEMENTS

This research was supported by TWAS-CNPq and Fapemig (EDT 01/2013). The authors are also grateful to TWAS-CNPq for awarding Adewale Adewuyi a postdoctoral fellowship at Universidade Federal de Minas Gerais, Minas Gerais, Brazil.

List of abbreviations and symbols

DSC	– differential scanning calorimetry
DTA	– differential thermal analysis
DTG	– derivative thermogravimetry
ECI	– empirical crystallinity index
FTIR	– Fourier transformed infrared spectroscopy
HS	– <i>Hibiscus sabdariffa</i> seed
HSC	– <i>Hibiscus sabdariffa</i> cellulose
HSM	– <i>Hibiscus sabdariffa</i> cellulose
OC	– oil holding capacity, ml g ⁻¹
SC	– swelling capacity, ml g ⁻¹
SEM	– scanning electron microscopy
TGA	– thermogravimetric analysis
TGA	– thermogravimetric analysis
WC	– water holding capacity, gg ⁻¹

XRD	– X-ray diffraction
A	– absorbance
c	– mass concentration, mg l ⁻¹
I	– diffraction intensity
I _c	– crystallinity index
m	– mass, g
q _e	– adsorption capacity, mg g ⁻¹
V	– volume, ml, l
W	– mass, g
θ	– diffraction angle, °

References

Literatura

1. M. A. S. Azizi Samir, F. Alloin, A. Dufresne, Review of recent research into cellulose whiskers, their properties and their application in nanocomposite field, *Biomacromolecules* **6** (2) (2005) 612–626, doi: <https://doi.org/10.1021/bm0493685>.
2. J. Kim, S. Yun, Z. Ounaies, Discovery of cellulose as a smart material, *Macromol.* **39** (2006) 4202–4206, doi: <https://doi.org/10.1021/ma060261e>.
3. N. N. Potter, J. H. Hotchkiss, *Food science*, fifth edition: Chapman and Hall, New York, 1995, pp. 24–68, doi: <https://doi.org/10.1007/978-1-4615-4985-7>.
4. T. Tseng, T. Kao, C. Chu, F. Chou, W. Lin, C. Wang, Induction of apoptosis by hibiscus protocatechuic acid in human leukemia cells via reduction of retinoblastoma (RB) phosphorylation and Bcl-2 expression, *Biochem. Pharmacol.* **60** (2000) 307–315, doi: [https://doi.org/10.1016/S0006-2952\(00\)00322-1](https://doi.org/10.1016/S0006-2952(00)00322-1).
5. M. H. El-Sherif, M. I. Sarwat, Physiological and chemical variations in producing roselle plant (*Hibiscus sabdariffa* L.) by using some organic farmyard manure, *World J. Agric. Sci.* **3** (5) (2007) 609–616, url: [https://www.idosi.org/wjas/wjas3\(5\)/10.pdf](https://www.idosi.org/wjas/wjas3(5)/10.pdf).
6. M. B. Atta, K. Imaizumi, Some characteristics of crude oil extracted from Roselle (*Hibiscus sabdariffa* L.) seeds cultivated in Egypt, *J. Oleo. Sci.* **51** (7) (2002) 457–461, doi: <https://doi.org/10.5650/jos.51.457>.
7. B. B. Mohamed, A. A. Sulaiman, A. A. Dahab, Roselle (*Hibiscus sabdariffa* L.) in Sudan, Cultivation and their uses, *Bull. Environ. Pharmacol. Life Sci.* **1** (6) (2012) 48–54, url: <http://bepls.com/may2012/10.pdf>.
8. T. Isogai, T. Saito, A. Isogai, Wood cellulose nanofibrils prepared by TEMPO electro-mediated oxidation, *Cellulose* **18** (2) (2011) 421–431, doi: <https://doi.org/10.1007/s10570-010-9484-9>.
9. K. Uetani, H. Yano, Nanofibrillation of wood pulp using a high-speed blender, *Biomacromolecules* **12** (2) (2011) 348–353, doi: <https://doi.org/10.1021/bm101103p>.
10. J. Zhang, H. Song, L. Lin, J. Zhuang, C. Pang, S. Liu, Microfibrillated cellulose from bamboo pulp and its properties. *Biomass and Bioenergy* **39** (2012) 78–83, doi: <https://doi.org/10.1016/j.biombioe.2010.06.013>.
11. G. Gürdag, S. Sarmad, Cellulose graft copolymers: Synthesis, properties, and applications, in: *Polysaccharide based graft copolymers*, Springer, 2013, doi: https://doi.org/10.1007/978-3-642-36566-9_2.
12. F. Khan, Photoinduced graft-copolymer synthesis and characterization of methacrylic acid onto natural biodegradable lignocellulose fiber, *Biomacromolecules* **5** (2004) 1078–1088, doi: <https://doi.org/10.1021/bm049967b>.
13. D. Roy, M. Semsarilar, J. T. Guthrie, S. Perrier, Cellulose modification by polymer grafting: a review, *Chem. Soc. Rev.* **38** (2009) 2046–2064, doi: <https://doi.org/10.1039/b808639g>.
14. A. Hebeish, J. T. Guthrie, *The chemistry and technology of cellulosic copolymers*, Springer, New York, NY, 1981, doi: <https://doi.org/10.1007/978-3-642-67707-6>.
15. D. Wang, J. Tan, H. Kang, L. Ma, X. Jin, R. Liu, Y. Huang, Synthesis, self-assembly and drug release behaviors of pH-responsive copolymers ethyl cellulose-graft-PDEAEMA through ATRP, *Carbohydr. Polym.* **84** (2011) 195–202, doi: <https://doi.org/10.1016/j.carbpol.2010.11.023>.
16. A. Carlmark, E. Larsson, E. Malmström, Grafting of cellulose by ring-opening polymerisation – A review, *Eur. Polym. J.* **48** (2012) 1646–1659, doi: <https://doi.org/10.1016/j.eurpolymj.2012.06.013>.
17. R. Khullar, V. K. Varshney, S. Naithani, P. L. Soni, Grafting of acrylonitrile onto cellulosic material derived from bamboo (*Dendrocalamus strictus*), *eXPRESS Polym. Lett.* **2** (1) (2008) 12–18, doi: <https://doi.org/10.3144/expresspolymlett.2008.3>.
18. A. Adewuyi, R. A. Oderinde, B. V. S. K. Rao, R. B. N. Prasad, B. Anjaneyulu, *Blighia unijugata* and *Luffa cylindrica* seed oils: Renewable sources of energy for sustainable development in rural Africa, *BioEner. Res.* **5** (2012) 713–718, doi: <https://doi.org/10.1007/s12155-012-9180-8>.
19. W. P. Flauzino Neto, H. A. Silvério, N. O. Dantas, D. Pasquini, Extraction and characterization of cellulose nanocrystals from agro-industrial residue – Soy hulls, *Ind. Crops Prod.* **42** (2013) 480–488, doi: <https://doi.org/10.1016/j.indcrop.2012.06.041>.
20. M. Zhang, C. J. Zhang, S. Shrestha, Study on the preparation technology of superfine ground powder of *Agroclybe chaxingu* Huang, *J. Food. Eng.* **67** (2005) 333–337, doi: <https://doi.org/10.1016/j.jfoodeng.2004.04.036>.
21. H. Lu, Y. Gui, L. Zheng, X. Liu, Morphological, crystalline, thermal and physicochemical properties of cellulose nanocrystals obtained from sweet potato residue, *Food Res. Int.* **50** (2013) 121–128, doi: <https://doi.org/10.1016/j.foodres.2012.10.013>.
22. E. Lecumberri, R. Mateos, M. Izquierdo-Pulido, P. Rupérez, L. Goya, L. Bravo, Dietary fibre composition, antioxidant capacity and physico-chemical properties of a fibre-rich product from cocoa (*Theobroma cacao* L.), *Food Chem.* **104** (2007) 948–954, doi: <https://doi.org/10.1016/j.foodchem.2006.12.054>.
23. K. K. Pandey, A. J. Pitman, FTIR studies of the changes in wood chemistry following Decay by brown-rot and white-rot fungi, *Int. Biodeterior. Biodegrad.* **52** (2003) 151–160, doi: [https://doi.org/10.1016/S0964-8305\(03\)00052-0](https://doi.org/10.1016/S0964-8305(03)00052-0).
24. E. A. Abdel-Razik, Aspects of thermal graft copolymerization of methyl methacrylate onto ethyl cellulose in homogeneous media, *Polym. Plast. Technol. Eng.* **36** (1997) 891–903, doi: <https://doi.org/10.1080/03602559708000668>.
25. D. Roy, J. T. Guthrie, S. Perrier, Graft polymerization: grafting poly(styrene) from cellulose via reversible addition-fragmentation chain transfer (RAFT) polymerization, *Macromol.* **38** (2005) 10363–10372, doi: <https://doi.org/10.1021/ma0515026>.
26. N. A. Rosli, I. Ahmed, I. Abdullah, Isolation and characterization of cellulose nanocrystals from *Agave angustifolia* fibre, *BioResources* **8** (2013) 1893–1908, doi: <https://doi.org/10.15376/biores.8.2.1893-1908>.
27. M. Troedec, D. Sedan, C. Peyratout, J. Bonnet, A. Smith, R.

- Guinebretiere, V. Gloaguen, P. Krausz, Influence of various chemical treatments on the composition and structure of hemp fibers, *Compos. Part A-Appl. S.* **39** (3) (2008) 514–522.
28. A. Mandal, D. Chakrabarty, Isolation of nanocellulose from waste sugarcane bagasse (SCB) and its characterization, *Carbohydr. Polym.* **86** (2011) 1291–1299, doi: <https://doi.org/10.1016/j.carbpol.2011.06.030>.
29. D. Ciolacu, F. Ciolacu, V. I. Popa, Amorphous cellulose-Structure and characterization, *Cellulose Chem Technol.* **45** (1-2) (2011) 13–21.
30. M. L. Nelson, R. T. O'Connor, Relation of certain infrared bands to cellulose crystallinity and crystal lattice type. Part II. A new infrared ratio for estimation of crystallinity in cellulose I and II, *J. Appl. Polym. Sci.* **8** (1964) 1325–1341, doi: <https://doi.org/10.1002/app.1964.070080323>.
31. M. Poletto, H. L. Ornaghi Jr, A. J. Zattera, Native cellulose: Structure, characterization and thermal properties, *Materials* **7** (2014) 6105–6119, doi: <https://doi.org/10.3390/ma7096105>.
32. W. S. Chen, H. P. Yu, Y. X. Liu, P. Chen, M. X. Zhang, Y. F. Hai, Individualization of cellulose nanofibers from wood using high-intensity ultrasonication combined with chemical pre-treatments, *Carbohydr. Polym.* **83** (4) (2011) 1804–1811, doi: <https://doi.org/10.1016/j.carbpol.2010.10.040>.
33. P. Lu, Y. L. Hsieh, Preparation and properties of cellulose nanocrystals: Rods, spheres, and network, *Carbohydr. Polym.* **82** (2010) 329–336, doi: <https://doi.org/10.1016/j.carbpol.2010.04.073>.
34. H. Lu, Y. Gui, L. Zheng, X. Liu, Morphological, crystalline, thermal and physicochemical properties of cellulose nanocrystals obtained from sweet potato residue, *Food Res. Inter.* **50** (2013) 121–128, doi: <https://doi.org/10.1016/j.foodres.2012.10.013>.
35. M. Mucha, S. Ludwiczak, M. Kawinska, Kinetics of water sorption by chitosan and its blends with poly(vinyl alcohol), *Carbohydr. Polym.* **62** (1) (2005) 42–49, doi: <https://doi.org/10.1016/j.carbpol.2005.07.008>.
36. N. M. Zain, S. M. Yusop, I. Ahmad, Preparation and characterization of cellulose and nanocellulose from Pomelo (*Citrus grandis*) Albedo, *J. Nutr. Food Sci.* **5** (2014) 1–4, doi: <https://doi.org/10.4236/jns.2014.51001>.
37. B. J. Kirby, *Micro and nanoscale fluid mechanics: Transport in microfluidic devices*, Cambridge University Press, 2010, doi: <https://doi.org/10.1017/CBO9780511760723>.
38. D. A. H. Hanaor, M. Michelazzi, C. Leonelli, C. C. Sorrell, The effects of carboxylic acids on the aqueous dispersion and electrophoretic deposition of ZrO₂, *J. Eur. Ceram. Soc.* **32** (1) (2012) 235–244, doi: <https://doi.org/10.1016/j.jeurceramsoc.2011.08.015>.
39. B. Salopek, D. Krasic, S. Filipovic, Measurement and application of zeta-potential, *Rudarsko-geolosko-naftni zbornik* **4** (1992) 147–151.
40. G. S. Chauhan, S. Bhatt, I. Kaur, A. S. Singha, B. S. Kaith, Modification of natural polymers: graft copolymers of methyl methacrylate onto rayon fibre initiated by ceric ions- A study in the swelling and thermal properties, *J. Polym. Mater.* **16** (1999) 245–252, url: [http://nopr.niscair.res.in/bitstream/123456789/23611/1/IJFTR%2024\(4\)%20269-275.pdf](http://nopr.niscair.res.in/bitstream/123456789/23611/1/IJFTR%2024(4)%20269-275.pdf).
41. G. S. Chauhan, S. S. Bhatt, I. Kaur, B. S. Kaith, A. S. Singha, Evaluation of optimum grafting parameters and the effect of ceric ion initiated grafting of methyl methacrylate onto jute fibre on the kinetics of thermal degradation and swelling behavior, *Polym. Degrad. Stab.* **69** (2000) 261–265, doi: [https://doi.org/10.1016/S0141-3910\(00\)00063-X](https://doi.org/10.1016/S0141-3910(00)00063-X).
42. R. K. Sharma, A study in thermal properties of graft copolymers of cellulose and methacrylates, *Adv. Appl. Sci. Res.* **3** (6) (2012) 3961–3969, url: <http://www.imedpub.com/articles/a-study-in-thermal-properties-of-graft-copolymers-of-cellulose-andmethacrylates.pdf>.
43. M. Carrier, A. Loppinet-Serani, D. Denux, J. M. Lasnier, F. Ham-Pichavant, F. Cansell, C. Aymonier, Thermogravimetric analysis as a new method to determine the lignocellulosic composition of biomass, *Biomass and Bioenergy* **35** (1) (2011) 298–307, doi: <https://doi.org/10.1016/j.biombioe.2010.08.067>.
44. A. N. Shebani, A. J. van Reenen, M. Meincken, The effect of wood extractives on the thermal stability of different wood-LLDPE composites, *Thermochim. Acta* **481** (1-2) (2009) 52–56, doi: <https://doi.org/10.1016/j.tca.2008.10.008>.
45. M. E. Babiker, A. R. A. Aziz, M. Heikal, S. Yusup, M. Abakar, Pyrolysis characteristics of *Phoenix dactylifera* date palm seeds using thermo-gravimetric analysis (TGA), *Int. J. Environ. Sci. Dev.* **4** (5) (2013) 521–524, doi: <https://doi.org/10.7763/IJESD.2013.V4.406>.
46. J. Hong, S. Y. Zhang, Effect of ultra-fine pulverization by wet processing on particle structure and physical properties of soybean dietary fiber. (in Chinese), *J. China Agric. University* **10** (2005) 90–94.
47. N. Grigelmo-Miguel, O. Martin-Belloso, Comparison of dietary fibre from byproducts of processing fruits and greens and from cereals, *LWT – Food Sci. Technol.* **32** (1999) 503–508, doi: <https://doi.org/10.1006/fstl.1999.0587>.
48. C. G. De Kruijff, S. G. Anema, C. Zhu, P. Havea, C. Coker, Water holding capacity and swelling of casein hydrogels, *Food Hydrocoll.* **44** (2015) 372–379, doi: <https://doi.org/10.1016/j.foodhyd.2014.10.007>.
49. C. F. Chau, Y. T. Wang, Y. L. Wen, Different micronization methods significantly improve the functionality of carrot insoluble fibre, *Food Chem.* **100** (2007) 1402–1408, doi: <https://doi.org/10.1016/j.foodchem.2005.11.034>.
50. A. K. Biswas, V. Kumar, S. Bhosle, J. Sahoo, M. K. Chatli, Dietary fibre as functional ingredients in meat products and their role in human health, *Int. J. Livest. Prod.* **2** (4) (2009) 45–54.
51. L. L. W. C. Yalagama, D. N. Karunaratne, R. Sivakanesan, C. Jayasekara, Chemical and functional properties of fibre concentrates obtained from by-products of coconut kernel, *Food Chem.* **141** (2013) 124–130, doi: <https://doi.org/10.1016/j.foodchem.2013.02.118>.
52. H. Tizazu, S. A. Emire, Chemical composition, physico-chemical and functional properties of lupin (*Lupinus albus*) seeds grown in Ethiopia, *Afr. J. Food Agric. Nutr. Dev.* **10** (8) (2010) 3029–3046, doi: <https://doi.org/10.4314/ajfand.v10i8.60895>.
53. F. Rafieian, J. Keramat, M. Shahedi, Physicochemical properties of gelatin extracted from chicken deboner residue, *LWT – Food Sci. Technol.* **64** (2015) 1370–1375, doi: <https://doi.org/10.1016/j.lwt.2015.04.050>.
54. M. A. Shad, H. Nawaz, M. Noor, H. B. Ahmad, M. Husain, M. A. Choudhry, Functional properties of maize flour and its blends with wheat flour: Optimization of preparation conditions by response surface methodology, *Pak. J. Bot.* **45** (6) (2013) 2027–2035, doi: <https://doi.org/10.13140/2.1.4326.9760>.
55. A. I. Akinyede, I. A. Amoo, Chemical and functional properties of full fat and defatted *Cassia fistula* seed flours, *Pak. J. Nutr.* **8** (6) (2009) 765–769, doi: <https://doi.org/10.3923/pjn.2009.765.769>.
56. A. G. Nassar, A. A. Abdel-Hamied, E. A. El-Naggar, Effect of citrus by-products flour incorporation on chemical, rheologi-

- cal and organoleptic characteristics of biscuits, *World J. Agric. Sci.* **4** (5) (2008) 612–616, url: [http://www.idosi.org/wjas/wjas4\(5\)/14.pdf](http://www.idosi.org/wjas/wjas4(5)/14.pdf).
57. E. Aydin, D. Gocmen, The influences of drying method and metabisulfite pre-treatment on the color, functional properties and phenolic acids contents and bioaccessibility of pumpkin flour, *LWT – Food Sci. Technol.* **60** (2015) 385–392, doi: <https://doi.org/10.1016/j.lwt.2014.08.025>.
 58. M. S. Islam, M. K. Ahmed, M. Raknuzzaman, M. H. Mamun, M. K. Islam, Heavy metal pollution in surface water and sediment: A preliminary assessment of an urban river in a developing country, *Ecol. Indic.* **48** (2015) 282–291, doi: <https://doi.org/10.1016/j.ecolind.2014.08.016>.
 59. S. Su, R. Xiao, X. Mi, X. Xu, Z. Zhang, J. Wu, Spatial determinants of hazardous chemicals in surface water of Qiantang River, China. *Ecol. Indic.* **24** (2013) 375–381, doi: <https://doi.org/10.1016/j.ecolind.2012.07.015>.
 60. D. Tiwari, H. Kimb, S. Lee, Removal behavior of sericite for Cu(II) and Pb(II) from aqueous solutions: Batch and column studies, *Sep. Purif. Technol.* **57** (2007) 11–16, doi: <https://doi.org/10.1016/j.seppur.2007.03.005>.
 61. R. Wahj, Z. Ngaini, V. U. Jok, Removal of mercury, lead and copper from aqueous solution by activated carbon of palm oil empty fruit bunch, *World Appl. Sci. J.* **5** (2009) 84–91.
 62. M. Jiang, X. Jin, X. Lu, Z. Chen, Adsorption of Pb(II), Cd(II), Ni(II) and Cu(II) onto natural kaolinite clay, *Desalination* **252** (2010) 33–39, doi: <https://doi.org/10.1016/j.desal.2009.11.005>.
 63. W. P. Putra, A. Kamari, S. N. M. Yusoff, C. F. Ishak, A. Mohamed, N. Hashim, I. Md Isa, Biosorption of Cu(II), Pb(II) and Zn(II) ions from aqueous solutions using selected waste materials: Adsorption and characterisation studies, *J. Encaps. Adsorp. Sci.* **4** (2014) 25–35, doi: <https://doi.org/10.4236/jeas.2014.41004>.
 64. G. O. Adediran, A. C. Tella, H. A. Mohammed, Adsorption of Pb, Cd, Zn, Cu and Hg ions on formaldehyde and pyridine modified bean husks, *J. Appl. Sci. Environ. Manage.* **11** (2007) 153–158, doi: <https://doi.org/10.4314/jasem.v11i2.55019>.
 65. O. S. Lawal, A. R. Sannia, I. A. Ajayi, O. O. Rabi, Equilibrium, thermodynamic and kinetic studies for the biosorption of aqueous lead(II) ions onto the seed husk of *Calophyllum inophyllum*, *J. Hazard. Mat.* **177** (2010) 829–835, doi: <https://doi.org/10.1016/j.foodres.2012.09.044>.
 66. C. M. Futralan, W. Tsai, S. Lin, M. L. Dalida, M. Wan, Copper, nickel and lead adsorption from aqueous solution using chitosan-immobilized on bentonite in a ternary system. *Sustain, Environ. Res.* **22** (6) (2012) 345–355, url: <http://140.116.228.7/download/22-6/22-6-1.pdf>.
 67. A. F. Wells, *Structural Inorganic Chemistry*, 5th Ed., Clarendon Press, Oxford, 1984 pp. 1288.
 68. L. Menon, S. D. Majumdar, U. Ravi, Mango (*Mangifera indica* L.) kernel flour as a potential ingredient in the development of composite flour Bread, *Ind. J. Nat. Prod. Res.* **5** (1) (2014) 75–82.
 69. S. Ashraf, S. M. G. Saeed, S. A. Sayeed, R. Ali, Impact of microwave treatment on the functionality of cereals and legumes, *Int. J. Agric. Biol.* **14** (3) (2012) 365–370.
 70. V. Benítez, S. Cantera, Y. Aguilera, E. Mollá, R. M. Esteban, M. F. Díaz, M. A. Martín-Cabrejas, Impact of germination on starch, dietary fiber and physicochemical properties in non-conventional legumes, *Food Res. Int.* **50** (2013) 64–69, doi: <https://doi.org/10.1016/j.foodres.2012.09.044>.

SAŽETAK

Kemijska modifikacija površinskim cijepljenjem celuloze izolirane iz biljke *Hibiscus sabdariffa*: potencijalni bioizvor za industrijsku primjenu

Adewale Adewuyi^{a,b*} i Fabiano Vargas Pereira^b

Etilendiamin je cijepljen na celulozu biljke *Hibiscus sabdariffa* jednostavnim kemijskim procesom. Modificirana (HSM) i nemodificirana celuloza (HSC) okarakterizirane su infracrvenom spektroskopijom s Fourierovom transformacijom (FTIR), elementnom analizom, pretražnim elektronskim mikroskopom (SEM), rendgenskom difrakcijom (XRD), raspodjelom veličine čestica, zeta-potencijalom, termogravimetrijskom analizom (TGA) i diferencijalnom skenirajućom kalorimetrijom (DSC). Određeni su kapacitet zadržavanja vode, kapacitet zadržavanja ulja, kapacitet bubrenja i adsorpcija teških metala. Raspodjela veličine čestica HSC-a je monomodalna, dok je za HSM bila dvomodalna. HSM je pokazao bolje rezultate u odnosu na HSC u području kapaciteta adsorpcije ulja i kapaciteta za adsorpciju metala, posebice iona Pb^{2+} i Cd^{2+} . HSM također pokazuje bolja svojstva od nekih celuloznih materijala nađenih u literaturi. Temeljem tih svojstva, HSM predstavlja potencijalni izvor u prehrambenoj industriji te pri obradi vode zagađene teškim metalima.

Ključne riječi

Celuloza, etilendiamin, *Hibiscus sabdariffa*, modificirana celuloza, površinsko cijepljenje

^a Department of Chemical Sciences, Faculty of Natural Sciences, Redeemer's University, 110 115 Mowe, Ogun state, Nigerija

^b Department of Chemistry, Federal University of Minas Gerais, Av. Antônio Carlos, 6627, Pampulha, CEP 31270-901 Belo Horizonte, MG, Brazil

Izvorni znanstveni rad
Prispjelo 12. lipnja 2016.
Prihvaćeno 29. srpnja 2016.